Int. J. Electrochem. Sci., 17 **(2022)** Article Number: 221291, doi: 10.20964/2022.12.69

International Journal of
ELECTROCHEMICAL
SCIENCE
www.electrochemsci.org

Short Communication

Improved Thermoelectric Performance of Flexible Polypyrrole/Tellurium Flexible Films Prepared by Two-Step Electrochemical Deposition

Mengting Liu[1,2], *Meng Li*[2], *RongfangWu*[2], *Peipei Liu*[1,2,*], *Cheng Liu*[1,*]

[1] Department of Physics, Jiangxi Science & Technology Normal University, Nanchang, 330013, P.R. China.
[2] Jiangxi Key Laboratory of Flexible Electronics, Jiangxi Science & Technology Normal University, Nanchang, 330013, P.R. China
[*]E-mail: liupeipei8866@126.com; liucheng_8111@aliyun.com
Mengting Liu and Meng Li contributed equally to this work.

Received: 3 October 2022 / *Accepted:* 23 November 2022 / *Published:* 27 December 2022

Thermoelectric (TE) materials, which enable the converted heat into electricity, have attracted growing attention as an essential green energy. Organic TE material polypyrrole (PPy) is an attractive candidate, because of its intrinsic advantages including low toxicity, lightweight, and good environmental compatibility. However, its TE performance is still poor through adjusting the doping level, which hinders its further applications. Integrating pyrrole with inorganic TE materials can possess favorable synergistic effect, which is considered as an effective strategy to improve TE performance. In this work, PPy/Tellurium (Te) composite films were prepared by electrochemical deposition in H_2SO_4 and Na_2TeO_3 systems, and their TE properties were investigated. Consequently, the TE properties of the flexible composite PPy/Te film were optimized. The power factor (*PF*) is nearly 10 times higher than that of the PPy reaching 3.10 μW m^{-1} K^{-1} after 120 min of Te electrodeposition. When the deposition potential of Te is -0.8 V, the TE performance of the flexible PPy/Te film was further improved. The prepared films displayed a maximum *PF* of about 4.02 μW m^{-1} K^{-1}, which is much better than those of original PPy. All results demonstrate that it's a promising method for enhancing the TE performance of conducting polymer-based materials.

Keywords: polypyrrole, tellurium, thermoelectric, electrodeposition, composite films

1. INTRODUCTION

The greenhouse effect and energy crisis are common challenges to the survival and development of humanity. Therefore, developing environment-friendly technology and improving energy efficiency are vital ways to solve the aforementioned problems [1]. As a green energy

technology, thermoelectric (TE) materials get the increasing attention of researchers due to their advantages. TE materials can realize the direct or reversible conversion of thermal and electrical signals through the motion of carriers without noise during the process [2-4].

The performance of TE materials can be evaluated by the dimensionless value *ZT*, $ZT = S^2\sigma/\kappa$, where *S*, σ and κ represent the Seebeck coefficient, the electrical conductivity and the thermal conductivity, repectively [5]. High-performance of the TE materials require high Seebeck coefficients and electrical and low thermal conductivity. In fact, these parameters are correlated and determined by the material structure. However, *S*, σ, and κ, as the tuning of one may lead to a negative effect on another [6]. In addition, the value of thermal conductivity cannot be accurately obtained, therefore the power factor ($PF=S^2\sigma$) is usually used as an indicator for evaluating TE properties of the materials. Balancing between the electrical conductivity and Seebeck coefficient is key to achieving a high *PF* [7].

Conductive polymers as TE materials, such as polypyrrole [8], polyaniline [9], and polythiophene [10], which possess the attractive merits of being lightweight, low cost, and no gas emission, have drawn much attention. As one of the important conductive polymers applied in TE materials, PPy has been extensively investigated due to its unique features, including its low cost of raw materials, bio-compatibility, inexpensiveness, and distinguished environmental stability [11]. But the TE properties of PPy are lower than those of inorganic TE materials. Hence, much effort has been devoted to optimizing their TE properties, including enhancing the molecular chain order and controlling the doping level. It has achieved remarkable advancement through various optimization strategies [12-15]. Whereas, the TE performance of PPy by adjusting the doping level still exhibits lower energy conversion capacity, because of the relatively low value of σ and *S*, hindering their applications in practice.

Bi_2Te_3 [16], PbTe [17], and GeTe [18] as inorganic TE materials have been confirmed as competitive candidate. However, they are generally limited by the high processing costs, toxicity and brittleness. It is clearly to see that they belong to Te-based materials. It consists of helical chains of Te atoms and the bonds between atoms in the same chain are covalent. In addition, the interactions between the chains are thought to be a mixture of electronic and van der Waals forces[19, 20]. Te as one of p-type TE materials shows a narrow band gap and high Seebeck coefficient (408 $\mu V\ K^{-1}$) [21-23]. In recent years, Te is considered an emerging TE material and has been extensively applied in many fields such as thermoelectric generator and potassium-ion batteries.

Organic-inorganic hybrid composites have been widely recognized as a significant direction for the improvement of TE performance. The composite can take advantages of the high Seebeck coefficient of inorganic materials and the good mechanical flexibility of organic materials, which is considered to be an effective strategy. Because the interface effect will generate at the surface between organic and inorganic, enhancing the TE performance of the material. Specifically, the formation of nanoscaled interfaces can scatter phonons effectively, contributing to the improvement of the Seebeck coefficient [24]. In addition, these nanostructures can select out low-energy charge carriers at interfacial energy barriers, thereby suppressing κ ($< 1\ W\ m^{-1}\ K^{-1}$), which is a critical advantage for the improvement of *PF*. Thus, organic-inorganic composites play an essential role in realizing improvement in *PF*.

Evaporation, sputtering, and vapor deposition are common ways to deposit thin films. But they suffer from a strict environment and complicated process sequence, which is not suitable for large-scale preparation. In contrast, the electrodeposition method can control the thickness and oxidation degree of conducting polymers, and the tightness of the interface contact between various components, because of the adjusted the deposition potential, deposition time and electrolyte ion concentration [14, 25, 26]. More importantly, the combination of organic and inorganic components can be significantly driven by the electric field. Recently, there are a few reports on organic-inorganic hybrid composites via electrodeposition method. For instance, Dan reported that PEDOT nanowire film was used as a working electrode for electrodepositing Te. The *PF* of the flexible hybrid film reached to 240 μW m^{-1} K^{-1}, which was 8 times higher than that of the pristine PEDOT NW film 27. Mario successfully fabricated flexible Te/ PEDOT films by electrochemical method, achieving a high *PF* of 320 ± 16μW m^{-1} K^{-1} after 2.5 h 28. Li demonstrated the full-electrochemical method to prepare flexible PPy/Te hybrid films through sequentially depositing. Finally, the *PF* of PPy/Te films reached 234.3 ± 4.1 μW m^{-1} K^{-1} 29. The electrodeposition of Te over a conducting polymer film provides an effective strategy to improve the TE performance of flexible inorganic/organic materials. In our work, PPy is used as the working electrode during the electrodeposition of Te, which is desired to obtain high *PF* values without further steps in the synthesis process.

Herein, the flexible PPy/Te films were fabricated by two-step electrochemical polymerization. Free-standing PPy films were prepared as working electrodes during the electropolymerization of PPy/Te films. To optimize the TE properties of the prepared flexible film, the electrodeposition time of Te and the electrodeposition potential and is precisely regulated. The electrochemical results reveal that the prepared film displayed a maximum PF of about 4.02 μW m^{-1} K^{-1}, which is much better than those of original PPy.

2. EXPERIMENTAL

2.1. Materials

Pyrrole (Py, 98%) and Sodium tellurite (Na_2TeO_3, 99.99%) were purchased from J&K Scientific Ltd, Concentrated sulfuric acid (H_2SO_4, 95-98%). Hydrochloric acid (HCl) were obtained from Xilong Chemical Co. Ltd.

2.2. Preparation of PPy films and PPy/Te composites films

PPy films were fabricated according to previous reports [30, 31]. The detailed processes are as followings: (1) Distillation of pyrrole monomer for purification; (2) Preparation of electrolyte: purified pyrrole was mixed with 3 mL boron trifluoride ether, 12 mL isopropyl alcohol and 0.2835g pentaerythritol oxide to prepare an electrolyte solution with a concentration of 0.07M pentaerythritol

and a concentration of 0.05 M pyrrole; (3) The anode polarization curve (LSV) was scanned in the above combined solution, the potential window was 0-1.15V, the scanning rate was 10 mV/s; (4) Determine the polymerization potential of pyrrole according to the initial oxidation potential. PPy films were prepared by electrochemical polymerization for 40 min and electrodeposition in the above electrolyte solution with constant potential of 0.85V in a three-electrode system under nitrogen protection in ice water bath.

Flexible PPy/Te composite films were prepared in a mixed system of H_2SO_4 and Na_2TeO_3 through an electrochemical deposition technique. The detailed processes are as followings: (1) 0.0264 g sodium nitrite (Na_2TeO_3) was added to 0.1 M H_2SO_4 to prepare a mixed solution with a concentration of 0.01M; (2) Cyclic voltammetry was carried out in the above solution, with the potential window ranging from -0.8V to 1.2V and the scanning rate of 20mV/s, and then the deposition potential of Te was determined according to the peak potential of the reduction peak; (3) According to the potentials obtained above, electrochemical constant pressure method was used to prepare flexible PPy/Te composite films with PPy film as the working electrode, platinum sheet as the counterelectrode, Ag/AgCI as the reference electrode, under the condition of nitrogen protection in ice water bath. The polymerization time was 60 min, 120min, 150 min, 180 min, 240 min, respectively. After deposition, the PPy/Te films were transferred from the solution and washed thoroughly with isopropanol to remove impurities. Finally, the films were dried in a vacuum oven at 60 °C for 3 h.

2.3. Characterization

The crystal structure of the PPy/Te film was analyzed by X-ray diffractometer (XRD) at room temperature. The scanning electron microscopy (SEM) images of the prepared samples were studied to analyze the microstructure. EDS (Energy dispersive spectrometer) and X-ray photoelectron spectroscopy (XPS) were employed to analyze elements. The conventional four-point probe method was applied to measure the electrical conductivity (σ) of PPy films and PPy/Te films. The induced difference voltage (ΔV) at the ends of as-deposited PPy and PPy/Te films were measured by Keithley 2700. Temperature difference (ΔT) of 5 ± 0.5 K was set by an ohm resistive heater at the ends of PPy and PPy/Te films. The Seebeck coefficient was estimated by the following formula:

$$S = -\frac{\Delta V}{\Delta T}$$

3. RESULTS AND DISCUSSION

Cyclic voltammetric curve is used to control the redox peak potential of monomers in electrolyte solutions. As shown in Figure 1, cyclic voltammetric curve exhibits a typical intersection between the cathodic scan and the anodic scan, which is named a “nucleation loop” [28]. The appearance of a nucleation loop indicates that Te is formed and grown on the surface of electrodes [32].

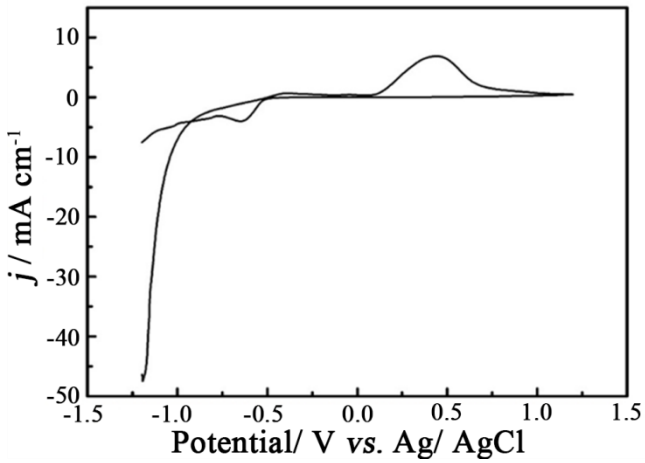

Figure 1. Cyclic voltammetric curve of Te in 0.1 M H_2SO_4, Scanning range: -1.2 ~1.2 V, Scanning rate: 20 mV s^{-1}.

Moreover, the reduction peak potential of Te is -0.67 V, which corresponds to the reaction shown in equation 1-1 [32, 33]. The peak potential of the oxidation peak is 0.47 V, and can be attributed to the oxidation of the bulk Te, which corresponds to the reaction shown in equations 1-2 [21, 34]. It is confirmed that Te can be electrodeposited in the above-mentioned H_2SO_4 and Na_2TeO_3 systems at a potential lower than -0.65 and the deposition potential was set at 0.7 V through cyclic voltammetric curve.

$$TeO_3^{2-} + 6H^+ + 4e^- \rightarrow Te + 3H_2O \quad (1\text{-}1)$$

$$Te + 2H^+ + 2e^- \rightarrow H_2Te \quad (1\text{-}2)$$

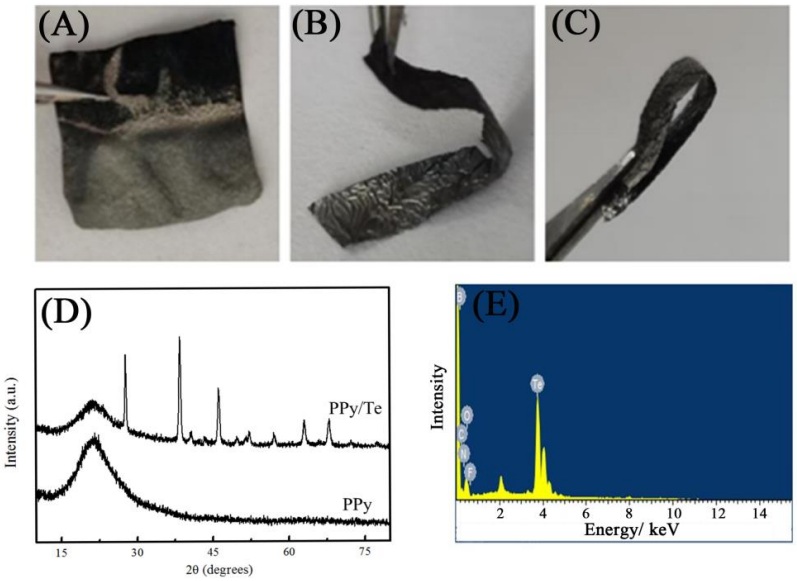

Figure 2. Digital images of PPy/Te films after (A) 60 min, (B) and (C)180 min of Te electrodeposition at -0.8 V; (D) XRD of PPy and PPy/Te films, (E) EDS analysis of PPy/Te films after 60 min of Te electrodeposition.

As shown in Figure 2A-C, the PPy/Te films exhibit high flexibility. The broad peak at 21.5° of Ppy can be attributed to the Miller surface (112) [36], as displayed in Figure 2D, which specifies that pure PPy has an amorphous non-crystalline structure [37, 39]. While, the peak of PPy/Te at 21.5° is wider than that of PPy, suggesting the reduced order of the composite film compared with that of the PPy film, which may be caused by the incorporation of Te [40]. For the PPy/Te films, the diffraction of (101), (102), and (003) planes centered at 28.6°, 38.1° and 43.8° can be observed, which are Te characteristic diffraction peaks of Te, manifesting that Te has been successfully electrodeposited on PPy electrodes[41, 42]. As shown in Figure 5E, a strong Te peak, as well as C, O, N, and F peaks were observed in the EDS spectrum of the PPy/Te flexible composite film, proving that Te is successfully deposited on the PPy film by the electrochemical method [41].

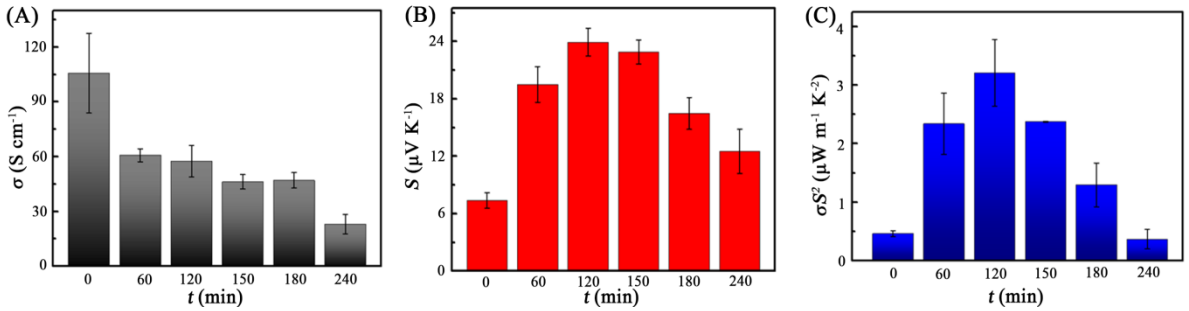

Figure 3. (A) Electrical conductivity, (B) Seebeck coefficient and (C) Power factor of PPy/Te films under various electrodeposition time.

Figure 3A shows the electrical conductivity of the prepared PPy/Te composite film in the H_2SO_4 and Na_2TeO_3 system with PPy film as the working electrode. Te is a kind of semiconductor with a high Seebeck coefficient and low conductivity. It can be seen that with the increase of electrochemical deposition time of Te, the electrical conductivity of the PPy/Te flexible composite film decreases linearly. The conductivity of the PPy film without Te deposition is 105 S cm^{-1}, while electrical conductivity of the PPy/Te flexible composite film decreased to 25 S cm^{-1} when the Te deposition time is 240 min. Many reasons resulted in the rapid decrease in conductivity. On the one hand, Te deposited by the electrochemical method is polycrystalline, leading to the PPy/Te composite film being porous, which affects its conductivity [32]. On the other hand, the deposition potential of Te is negative. The application of negative voltage for PPy films is de-doping[13, 35], resulting in a decrease in the doping level of the PPy film and a consequent decrease in the conductivity. Meanwhile, the conductivity of the pure PPy films are higher than that of Te, due to the higher doping level of PPy films obtained from electrochemical polymerization (0.85 V).

Figure 3B presents the Seebeck coefficient of the flexible PPy/Te composite film as a function of the deposition time of Te. The Seebeck coefficient first increases and then decreases with the increase of deposition time, which is consistent with that of the reported literature [27]. When the deposition time of Te is 120 min, the Seebeck coefficient of the PPy/Te film reached the maximum of 23μV K^{-1}, which is a threefold increase compared to pristine film. Therefore, it is supposed that Te

plays a decisive role in the Seebeck coefficient of flexible composites, that is, the addition of Te can significantly improve the Seebeck coefficient of PPy materials. The reasons for the high values of the prepared flexible composites are analyzed as follows: (1) The uniform and dense coating of Te on the surface of PPy, and the two components formed favorable interfacial contact, resulting in efficient energy filtering. The energy filtering effect can not only hinder the transmission of low-energy carriers to a certain extent, but also does not influence the transmission of high-energy carriers, which would be beneficial for the improvement of the Seebeck coefficient [10, 36]. (2) Te is a semiconductor with a high Seebeck coefficient. Therefore, the Seebeck coefficient of the flexible PPy/Te composite is higher that of the pure PPy film after electrochemical dedoping. (3) The cyclic voltammetric has confirmed that TeO_3^{2-} can be successfully reduced to Te under conditions below -0.67 V. The application of a negative potential is de-doping for the PPy film, that is, the electrodeposition of Te is accompanied by the de-doping process of PPy. De-doping can lead to a decline in the doping level of the PPy film, resulting in a decrease of carrier concentration and conductivity, and a increase of the Seebeck coefficient. When the deposition time exceeds 120 min, part of the Te may fall off, causing the decrease of the interface effect and the Seebeck coefficient.

The power factor of the composite film first increases and then decreases with the increase of Te deposition time, as displayed in Figure3C. The thermoelectric properties of the PPy/Te flexible composite films are dominated by the Seebeck coefficient, so the trend of the power factor is the same as that of the Seebeck coefficient. It can be seen that the optimal deposition time is 120 min, and the power factor reaches the maximum value of 3.1 μW m^{-1} K^{-1}, which is nearly 6 times higher than that of the prepared PPy film, implying the energy filtering effect between polypyrrole and Te.

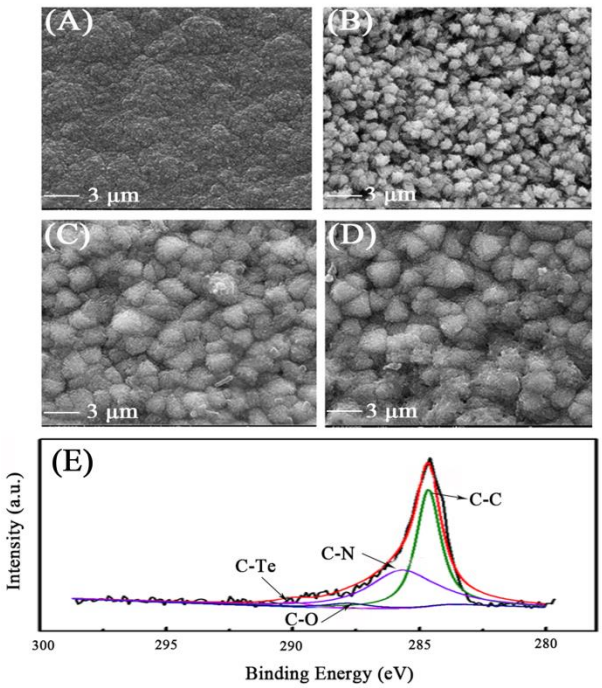

Figure 4. SEM images of (A) the pristine PPy film, (B) PPy/Te films after 60 min, (C) 120 min, (D) 180 min of Te electrodeposition. (E) XPS C1s spectra of PPy/Te films after 180 min of Te electrodeposition.

The surface morphology of PPy and PPy/Te film were investigated by SEM, as illustrated in Figure 4. The pure PPy film possesses a dense structure with numerous cauliflower-like granules. The changes of morphology of the composite films suggest that Te (hexagonal crystal structure) is successfully deposited on the surface of PPy without obvious agglomeration. As observed, the Te nanoparticles appear bright in colorer compared to pure PPy, which may result from the higher electron density on of Te than that of Ppy. Especially, the interaction between the van der Waals force of Te atoms and π interaction of PPy chains at the interface of PPy/Te generates an interfacial adhesion. Meanwhile, the PPy can hinder the passivation of Te particles on its surface and prevent oxidation during processing. In addition, abundant nano-interfaces between PPy and Te can generate an energy-filtering effect interface, which are beneficial to improve the TE performance.

The chemical composition of the film is analyzed by the XPS spectrum, as exhibited in Figure 4E. The characteristic peaks at 284.5 eV and 285.4 eV are assigned to C=C and C-C bonds, respectively. The peak of C-N at 284.4 eV can be attributed to the presence of PPy. The peak at 288.3 eV corresponds to the appearance of the C-Te peak, confirming the strong electronic coupling between PPy and Te, and further proving that Te is deposited on the PPy film, which are agree well with XRD and SEM analysis.

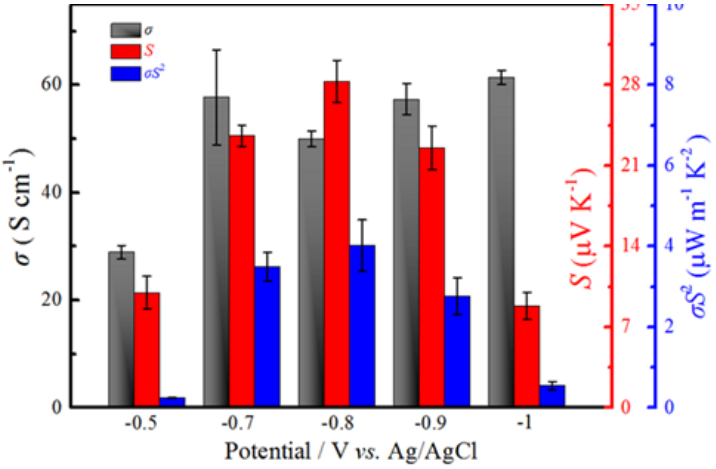

Figure 5. Electrical conductivity, Seebeck coefficient, power factor of PPy/Te films obtained under different electrodeposition potentials.

Figure 5 shows the conductivity, Seebeck coefficient, and power factor of the flexible PPy/Te composite film as a function of deposition potential. It is clear to see that the conductivity exhibits a trend of first increasing and then decreasing and then tend to stabilize under the potential range of -0.5 V ~ -1 V. The highest conductivity of the composite film is obtained when the deposition potential is 0.7 V. While the Seebeck coefficient shows a trend of first increasing and then decreasing, and the largest Seebeck coefficient and power factor reach to 29 μV K^{-1} and 4.02 μW m^{-1} K^{-1}at deposition potential of -0.8 V rather than a lower potential. This is because Te plays a crucial role in the Seebeck coefficient of the PPy/Te composite film. If the deposition potential of Te is low, part of Te will detach

from the PPy surface [38]. Thus the energy filtering effect at the interface of PPy and Te will be reduced, leading to the decrease of Seebeck coefficient energy.

4. CONCLUSION

In conclusion, a free-standing and flexible PPy/Te composite film was prepared by the electrodeposition method. The TE properties of the PPy/Te flexible composite films were systematically studied under the different deposition time and potential of Te. The results showed that the optimal deposition time and potential were 120 min and -0.8 V, respectively. The *PF* of the composite film reached 4.02 μW m^{-1} K^{-1}, which nearly 10 times higher than that of the pure PPy. The improvement of TE performance can be attributed to the energy filtering effect, which scattering of relatively low energy carriers by the barrier formed at the interface of Te and PPy. This study suggested that the prepared Ppy/Te film could be used as a promising candidate for high-performance TE system.

DECLARATION OF COMPETING INTEREST
There are no conflicts to declare.

ACKNOWLEDGEMENTS
This work was financially supported by the National Natural Science Foundation of China (52073128, 22065013), the Natural Science Foundation of Jiangxi Province, China (20202ACBL204005, 20202ACBL214005, 20212BAB214017, and 20203AEI003), Foundation of Jiangxi Science & Technology Normal University (2019BSQD001 and 3000990337).

References

1. B.C. Huo and C.Y. Guo, *Molecules*, 27 (2022) 6932.
2. C.J. An, Y.H. Kang, A.Y. Lee, K.S. Jang, Y. Jeong and S.Y. Cho, *ACS Appl. Mater. Interfaces*, 8 (2016) 22142.
3. A.F. Al Naim and A.G. El-Shamy, *Mat Sci Semicon Proc.*, 152 (2022) 107041.
4. M.S. Dresselhaus, G. Chen, M.Y. Tang, R.G. Yang, H. Lee, D.Z. Wang, Z.F. Ren, J.P. Fleurial and P. Gogna, *Adv. Mater.*, 19(2007) 1043.
5. J. Wang, K.F. Cai, S. Shen and J.L. Yin, *Synth. Met*., 195 (2014) 132.
6. M. Culebras, B. Uriol, C.M. Gomez and A. Cantarero, *Phys. Chem. Chem. Phys.*, 17 (2015) 15140.
7. T. Wu, X.L. Shi, W.D. Liu, S. Sun, Q.F. Liu and Z.G. Chen, *Macromol. Mater. Eng.*, (2022) 2200411.
8. J. Wu, Y. Sun, W.B. Pei, L. Huang, W. Xu and Q. Zhang, *Synth. Met.*, 196 (2014) 173.
9. J. Wu, Y. Sun, W. Xu and Q. Zhang, *Synth. Met.*, 189 (2014) 177.
10. L. Metref, A. Mekki, Z.B.D. Sayah, L. Nedjar, F. Delaleux, J.F. Durastanti and O. Riou, *Polymer Bull*, (2022) 1.
11. M. Bharti, A. Singh, S. Samanta and D.K. Aswal, *Prog. Mater Sci.*, 93 (2018) 270.
12. H.J. Goldsmid and R.W. Douglas, *Br. J. Appl. Phys.*, 5 (1954) 386.
13. F.R. Sie, H.J. Liu, C.H. Kuo, C.S. Hwang, Y.W. Chou and C.H. Yeh, *Intermetallics*, 92 (2018) 113.
14. M.C. Steele and F.D. Rosi, *J. Appl. Phys.*, 29 (1958) 1517.

15. G.C. Xi, Y.Y. Peng, W.C. Yu and Y. Qian, *Cryst Growth & Des.*, 5 (2005) 325.
16. Y.J. Zhu, W.W. Wang, R.J. Qi and X.L. Hu, *Angew. Chem.*, 116 (2004) 1434.
17. B. Abad, M. Rull-Bravo, S.L. Hodson, X.F. Xu and M. Martin-Gonzalez, *Electrochim. Acta*, 169 (2015) 37.
18. S. Lin, W. Li, Z. Chen, J. Shen, B. Ge and Y. Pei, *Nat Commun*, 7 (2016) 10287.
19. C. Dun, C.A. Hewitt, H.H. Huang, D.S. Montgomery, J.W. Xu and D.L. Carroll, *Phys. Chem. Chem. Phys.*, 17 (2015) 8591.
20. D. Vashaee and A. Shakouri, *Phys. Rev. Lett.*, 92 (2004) 106103.
21. Y. Hu, F. Jiang, B. Lu, C. Liu, J. Hou and J. Xu, *Electrochim. Acta*, 228 (2017) 361.
22. W. Yao, L. Shen, P. Liu,C. Liu, J. Xu, Q. Jiang, G. Liu, G. Nie and F, Jiang, *Mater. Chem. Front.*, 4 (2020) 597.
23. Y. Hu, D. Zhu, Z. Zhu, E. Liu, B. Lu, J. Xu, F. Zhao, J. Hou, H. Liu and F. Jiang, *Chemphyschem*, 17 (2016) 2256.
24. M. Li, F. Jiang, J. Yang, Y. Wang, F. Zhao, X. Xu, M. Liu, J. Yan and J.Xu, *ACS Appl. Energy Mater.*, 4 (2021) 12982.
25. M. Ma, L. Guo, D.G. Anderson and R. Langer, *Science*, 339 (2013) 186.
26. D. Grujicic and B. Pesic, *Electrochim. Acta*, 47 (2002) 2901.
27. D. Ni, H. Song, Y. Chen and K. Cai, *J. Materiomics*, 6 (2020) 364.
28. M. Culebras, A.M. Igual-Munoz, C. Rodriguez-Fernandez, M. Gomez-Gomez, C. Gomez and A. Cantarero, *ACS Appl. Mater. Interfaces*, 9 (2017) 20826.
29. Y. Li, C.Y. Gao, X.H. Fan and L.M. Yang, *ACS Appl. Mater. Interfaces*, 14 (2022) 10815.
30. Y. Fan, L. Jiang, J. Yang, Y. Jiang and F. Liu, *J. Electroanal. Chem.*, 771 (2016) 17.
31. Y. Mu, X. Gao, X. Zhou, H. Wang, P. Lv, M. Qiu and X. Zhang, *J. Alloys Compd.*, 765 (2018) 977.
32. M. Culebras, B. Uriol, C.M. Gómez and A. Cantarero, *Phys. Chem. Chem. Phys.*, 17 (2015) 15140.
33. M. Li, C. Luo, J. Zhang, J. Yang, J. Xu, W. Yao, R. Tan, X. Duan and F. Jiang, *Surf. Interfaces*, 21 (2020) 100759.
34. J. Zhou, H. Wang, D. He, Y. Zhou, W. Peng, F. Fan and H. Huang, *Appl. Phys. Lett.*, 112 (2018) 243904.
35. Debnath, K. Deb, K. Sarkar and B. Saha, *J. Phys. Chem. C*, 125 (2020) 168.
36. R. Kowalik, D. Kutyła, K. Mech and P. Zabinski, *Appl. Surf. Sci.*, 388 (2016) 817.
37. Q. Cheng, V. Pavlinek, C. Li, A. Lengalova, Y. He and P. Saha, *Appl. Surf. Sci.*, 253 (2006) 1736.
38. B. Yeole, T. Sen, D.P. Hansora and S. Mishra, *J. Appl. Polym. Sci.*, 132 (2015) 42379.
39. Q. Jiang, C. Liu, B. Lu, J. Xu, H. Song, H. Shi, D. Mo, Z. Wang, F. Jiang and Z. Zhu, *J. Mater. Sci.*, 50 (2015) 4813.
40. D. Park, H. Ju, T. Oh and J. Kim, *CrystEngComm*, 21 (2019) 1555.
41. Y. Wang, S.M. Zhang and Y. Deng, *J. Mater. Chem. A*, 4 (2016) 3554.
42. D. Wang, Q. Tian, L. Yang, S. Kuang, R. Jin, H. Yue, G. Wang, Q. Wang and S. Gao, *ChemistrySelect*, 4 (2019) 9737.